A new methodology development for flood fragility curve derivation considering structural deterioration for bridges

Jaebeom Lee[1], Young-Joo Lee[*1], Hyunjun Kim[1], Sung-Han Sim[1] and Jin-Man Kim[2]

[1]*School of Urban and Environmental Engineering, Ulsan National Institute of Science and Technology (UNIST), Ulsan, Korea*
[2]*Korea Institute of Construction Technology (KICT), Goyang-Si, Korea*

Abstract. Floods have been known to be one of the main causes of bridge collapse. Contrary to earthquakes, flood events tend to occur repeatedly and more frequently in rainfall areas; flood-induced damage and collapse account for a significant portion of disasters in many countries. Nevertheless, in contrast to extensive research on the seismic fragility analysis for civil infrastructure, relatively little attention has been devoted to the flood-related fragility. The present study proposes a novel methodology for deriving flood fragility curves for bridges. Fragility curves are generally derived by means of structural reliability analysis, and structural failure modes are defined as excessive demands of the displacement ductility of a bridge under increased water pressure resulting from debris accumulation and structural deterioration, which are known to be the primary causes of bridge failures during flood events. Since these bridge failure modes need to be analyzed through sophisticated structural analysis, flood fragility curve derivation that would require repeated finite element analyses may take a long time. To calculate the probability of flood-induced failure of bridges efficiently, in the proposed framework, the first order reliability method (FORM) is employed for reducing the required number of finite element analyses. In addition, two software packages specialized for reliability analysis and finite element analysis, FERUM (Finite Element Reliability Using MATLAB) and ABAQUS, are coupled so that they can exchange their inputs and outputs during structural reliability analysis, and a Python-based interface for FERUM and ABAQUS is newly developed to effectively coordinate the fragility analysis. The proposed framework of flood fragility analysis is applied to an actual reinforced concrete bridge in South Korea to demonstrate the detailed procedure of the approach.

Keywords: flood; fragility; debris; bridge; deterioration

1. Introduction

Bridges, which play an important role in our daily lives, are exposed to various extreme events and are known to be especially prone to flood-induced damage or destruction. A study by Wardhana and Hadipriono (2003), which investigated about 500 cases of bridge destruction that occurred in the USA between 1989 and 2000, revealed that flood-associated hydraulic factors, such as water pressure, scour, corrosion, and debris, are the most common causes of bridge

∗Corresponding author, Assistant Professor, E-mail: ylee@unist.ac.kr

destruction. For example, the hydrodynamic pressure generated by a rapid water flow because of flooding exerts pressure on the entire surface area of a bridge, and the debris accumulated around bridge piers increases the water pressure. This flood-induced load combined with in-service loading such as the bridge self-weight can cause structural damage or destruction. Without proper repair or reinforcement of such damaged or destroyed parts, the bridge would become even more susceptible to the flood hazard.

In addition, previous studies have confirmed that the uncertainty of a range of factors is involved in the flood-induced destruction of bridges. Several hydraulic characteristics have been reported to have uncertainty that should be considered while designing waterways or waterfront structures (Johnson 1996). Accordingly, many studies have performed numerical analyses of flood-related uncertainty factors such as the flow velocity and rate, water depth, and the geometric shapes and material properties of bridges (Johnson and Dock 1998, Ghosn *et al.* 2003).

In this context, several researchers have raised the issue of a need for research on the fragility curves typically associated with the structural vulnerability of bridges subjected to flood events. A fragility curve represents the probability of a structure incurring structural damage that exceeds a certain level as a result of being subjected to various degrees of extreme events. Much more research efforts have been devoted to seismic fragility analysis than to flood fragility analysis. As a result, seismic fragility curves are being widely used for seismic risk assessment and damage estimation as well as for establishing countermeasures.

In contrast, only a few works have studied the derivation of flood fragility curves. Decò and Frangopol (2011) derived the fragility curves for bridges by taking into account earthquakes, scour, and dynamic loading. Dong *et al.* (2013) derived seismic fragility curves that reflect the influences of scour and corrosion. Dawson *et al.* (2005) assessed the flood risk vulnerability of a fluvial dike system. Witzany and Cejka (2007) performed a numerical analysis of flood fragility of a stone vault bridge structure. However, these studies investigated hydraulic factors to consider the effects of only scour or corrosion for deriving seismic fragility curves, and they aimed to derive the flood fragility curves for non-bridge structures or a bridge having a specific geometric shape. Furthermore, as mentioned earlier, the hydraulic factors other than scour and corrosion, e.g., water pressure and debris, should also be considered while analyzing flood fragility in order to assess the flood fragility of common bridges.

This study therefore proposes a new methodology for deriving the flood fragility curves of bridges. A fragility curve is generally derived by means of structural reliability analysis requiring repeated structural analyses. Each of these structural analyses can be time-consuming if various hydraulic factors are considered in sophisticated structural analysis such as finite element analysis, and the time costs for deriving the flood fragility curves can be extremely high in the case of complicated bridge structures. To overcome these problems and to reduce the required number of structural analyses, in the proposed framework, the first order reliability method (FORM) is introduced into reliability analysis, which enables to perform the fragility analysis of bridges more efficiently. In addition, two software packages, which are respectively specialized for reliability analysis and finite element analysis, FERUM (Finite Element Reliability Using MATLAB) and ABAQUS, are coupled so that they can communicate with each other by exchanging their inputs and outputs during structural reliability analysis, and a Python-based software application is developed to effectively coordinate the communication.

2. Reliability analysis method

Fragility analysis requires reliability analysis for calculating the probability of an event in which a structure undergoes a certain level of damage. A number of reliability analysis methods have been developed and adopted for various engineering problems (Haldar 2006), and these methods can be categorized into two groups: sampling-based methods and analytical (or non-sampling-based) methods (Lee and Moon 2014). Representative types of these two groups include the Monte Carlo simulation (MCS) and the first order reliability method (FORM), respectively. Melchers (1999) and Der Kiureghian (2005) provided detailed reviews of these two methods. As mentioned above, the derivation of the fragility curve of a bridge subjected to a flood event requires repeated finite element analyses. Lee and Moon (2014) proved that FORM is a more efficient and appropriate method than the MCS for performing reliability analysis in conjunction with sophisticated finite element analysis; therefore, in this paper, FORM is employed to conduct reliability analysis for the derivation of flood fragility curves. The method is briefly summarized in this section, and further details can be found in Der Kiureghian (2005).

In structural reliability analysis, an event is generally defined as the incident wherein a structure undergoes a certain level of damage. The criterion for determining its structural damage, however, depends on the purpose of analysis: inordinate displacement, velocity or acceleration, and excessive strain. The analytical functions representing the structural damage states are called limit-state functions. In a structural reliability problem, a limit-state function is denoted by $g(\mathbf{x})$ and the event of interest (often called "failure") is expressed by $g(\mathbf{x}) \leq 0$ where $\mathbf{x}$ is a column vector of n random variables (RVs), i.e., $\mathbf{x} = [x_1, x_2,..., x_n]^{\mathrm{T}}$, representing the uncertainties in the given problem. Then the probability of the event P_f is

$$P_f = P[g(\mathbf{x}) \leq 0] = \int_{g(\mathbf{x}) \leq 0} f_{\mathbf{x}}(\mathbf{x}) d\mathbf{x} \tag{1}$$

where $f_{\mathbf{x}}(\mathbf{x})$ is the joint probability density function (PDF) of $\mathbf{x}$. Through transformation of the space of RVs into the standard normal space, the probability P_f can be expressed as

$$P_f = \int_{g(\mathbf{x}) \leq 0} f_{\mathbf{x}}(\mathbf{x}) d\mathbf{x} = \int_{G(\mathbf{u}) \leq 0} \phi_n(\mathbf{u}) d\mathbf{u} \tag{2}$$

where $G(\mathbf{u}) = g(\mathbf{T}^{-1}(\mathbf{u}))$ is the transformed limit-state function in the standard normal space, $\varphi_n(\cdot)$ is the n-th order standard normal PDF, $\mathbf{u}$ is the column vector of n standard normal variables, and $\mathbf{T}$ is the one-to-one mapping transformation matrix that satisfies $\mathbf{u} = \mathbf{T}(\mathbf{x})$.

In FORM, the probability (i.e., P_f in Eq. (2)) can be approximated by linearizing the function $G(\mathbf{u})$ at a point $\mathbf{u}^*$ that is defined by the following constrained optimization problem

$$\mathbf{u}^* = \arg \min \{\|\mathbf{u}\| \mid G(\mathbf{u}) = 0\} \tag{3}$$

where "arg min" denotes the argument of the minimum of a function and $\|\cdot\|$ is the L^2-norm. In Eq. (3), it is seen that $\mathbf{u}^*$ is located on the limit-state surface satisfying $G(\mathbf{u}) = 0$, and it is at a minimum distance from the origin in the standard normal space. As an example of the first-order approximation concept of FORM, Fig. 1 shows the approximated limit-state function in two-dimensional space.
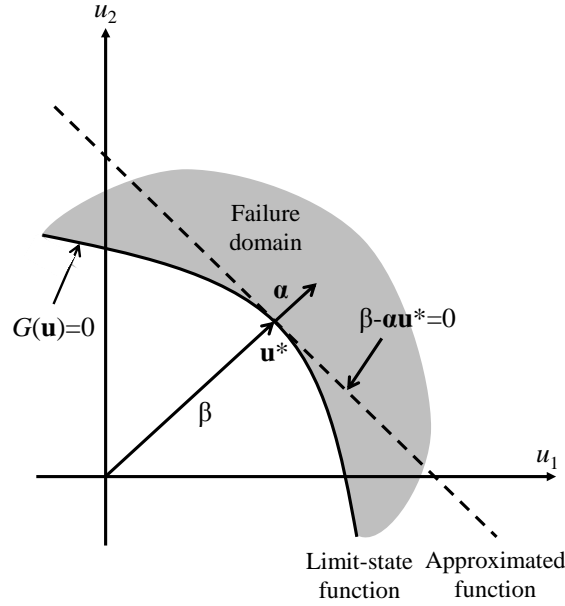
Fig. 1 Linear approximation in FORM

In the standard normal space shown in the figure, since equal probability density contours are concentric circles centered at the origin, $\mathbf{u^*}$ has the highest probability among all of the nodes in the failure domain, $G(\mathbf{u}) \leq 0$. In this sense, $\mathbf{u^*}$ is an optimal point and is commonly called the design point or the most probable point (MPP).

In consideration of the fact that $G(\mathbf{u^*})=0$, the limit-state function approximated at MPP is written as

$$G(\mathbf{u}) \cong \nabla G(\mathbf{u^*})(\mathbf{u}-\mathbf{u^*}) = \left\| \nabla G(\mathbf{u^*}) \right\| (\beta - \boldsymbol{\alpha}\mathbf{u}) \tag{4}$$

where $\triangledown G(\mathbf{u})=[\partial G/\partial u_1,\dots, \partial G/\partial u_n]$ denotes the gradient vector, $\boldsymbol{\alpha}=-\triangledown G(\mathbf{u^*})/\|\triangledown G(\mathbf{u^*})\|$ is the normalized negative gradient vector at the MPP (i.e., a unit vector normal to the limit-state surface at the MPP), and $\beta=-\boldsymbol{\alpha}\mathbf{u^*}$ is the reliability index. Then the first-order failure probability P_f is defined by the reliability index, i.e.

$$P_f \approx \Phi(-\beta) \tag{5}$$

where $\Phi(\cdot)$ denotes the standard normal cumulative distribution function (CDF).

One of the representative methods to solve the constrained optimization problem in Eq. (3) is the Hasofer-Lind Rackwitz-Fiessler (HL-RF) algorithm summarized in Fig. 2. Details of the algorithm and FORM can be found in Rackwitz and Fiessler (1978) and Der Kiureghian (2005). In the following numerical example, ε_1, ε_2, and i_{max} are assumed to be 0.01, 0.01, and 100, respectively.
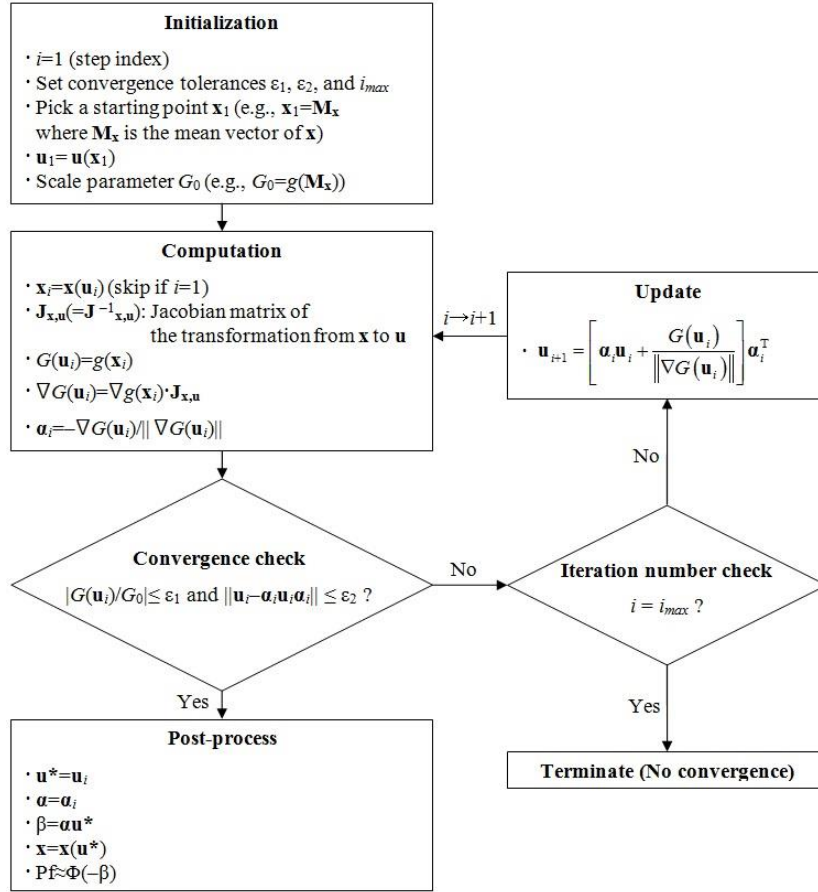
Fig. 2 FORM by HL-RF algorithm (Song 2007, Lee and Moon 2014)

3. Proposed framework for flood fragility analysis

3.1 Failure modes

A fragility curve is the relationship between the probability of failure and an intensity measure of a hazard. In seismic fragility analysis, the primary failure mode is generally defined as excessive stress or displacement greater than given thresholds resulting from earthquake-induced loadings. The intensity measure of loading is selected as either the peak ground acceleration or spectral acceleration, and the failure probabilities are described as dependent variables of the intensity measure in the fragility curve. Similarly, the failure mode and the intensity measure need to be defined for the case of floods because there are several different failure modes and flood intensity-related factors.

This study considers failure modes due to increased water pressure resulting from debris accumulation as well as decreased structural resistance resulting from corrosion, which are known as the primary causes of bridge failures during flood events (Schmocker and Hager 2011). While

scour is also an important hydraulic cause of bridge failures, its consideration requires in-depth understanding of soil-structure interactions and a specialized finite element model. This study focuses only on these debris- and corrosion-related failure modes, for the simplicity of describing the proposed fragility analysis framework. For scour-dominant bridges, however, scour can also be included as a failure mode within the proposed framework.

In bridge design, one of the critical water loads is stream pressure. AASHTO (2012) defines this water pressure as the pressure of flowing water acting in the longitudinal direction of bridge substructures, such as piers. Floating debris accumulates around piers and decks, resulting in increased water pressure on the bridge and frequent overflow that may induce secondary flood damage. AASHTO (2012) also suggests the effect of piled debris on the water force as a function of mean flow velocity. In that sense, the water velocity is introduced as a reasonable intensity measure to determine the bridge failure in this study. The water level may also be an appropriate intensity measure, but it is introduced as a deterministic parameter with its maximum value because it is assumed in this study that a bridge is in a severe flood and the water level reaches the level of girders.

According to AASHTO (2012) and KHBDS (Korean Highway Bridge Design Specification, 2010), water pressure and debris are usually considered together because the debris that accumulate around piers over time increases the water pressure. Section 3.7.3.1 of AASHTO (2012) provides an equation for the water pressure generated by dynamic water flow in US customary units. Conversion of this equation to SI units gives the water pressure p (MPa) as

$$p = 5.14 \times 10^{-4} C_D V^2 \tag{6}$$

where C_D denotes the drag coefficient for piers, whose values are specified in Table 1, and V denotes the flow velocity [m/s] during a flood. The drag coefficient depends on the geometric shape of the bridge and the accumulated debris or absence thereof as shown in Table 1, and the force exerted on the bridge is determined by multiplying the calculated hydrodynamic pressure by the projected area subjected to the pressure.

Lastly, the collision force by floating debris is also a considerable cause of bridge failures, but a preliminary analysis employing the mean values of RVs revealed that the impact of the collision force was relatively small, compared with the one of water pressure. Furthermore, the recent versions of AASHTO and KHBDS do not address the collision force in their bridge design guidelines anymore. For these reasons, the collision force by floating debris is not considered in this study.

Table 1 Drag coefficient

Type	C_D
Semicircular-nosed pier	0.7
Square-ended pier	1.4
Debris lodged against the pier	1.4
Wedged-nosed pier with nose angle 90 degrees or less	0.8

3.2 Structural deterioration and material nonlinearity

In this study, the water pressure rise caused by debris accumulation and the material deterioration caused by corrosion are considered as the governing factors during a flood event. If a bridge is used for a prolonged period without appropriate repair and retrofit, corrosion can occur locally in the damaged parts, resulting in structural deterioration, which makes it more prone to be damaged during floods. Moreover, water pressure generated by the rapid flow of water is exerted on the exposed surface area of the bridge, and the debris accumulated around bridge piers is an additional factor that increases the water pressure during floods. If the thus-increased water pressure acts on the bridge, the piers and girders are subjected to stress levels that exceed their yield stresses, resulting in a rapid increase in displacement, thereby showing spontaneous nonlinear behaviors of materials. Therefore, to achieve the derivation of an accurate flood fragility curve, such corrosion, water pressure and debris, as well as the nonlinear behaviors of materials should be modeled for finite element analysis.

Steel reinforcement bars suffer from corrosion, which is one of the major causes of bridge deterioration (Vu and Stewart 2000). Corrosion occurs when the hydroxide ions present in water infiltrate the concrete cover and come into contact with steel reinforcements. Corrosion deteriorates structures by decreasing their effective area and thus reducing their stiffness. Thoft–Christensen *et al.* (1997) proposed a time-dependent reduction in the cross sectional area of a steel reinforcement bar as follows (Dong *et al.* 2003)

$$A(t) = \begin{cases} \dfrac{\pi}{4} D_i^2 & \left(\text{for } t \leq T_i \right) \\[2mm] \dfrac{\pi}{4} \left[D(t) \right]^2 & \left(\text{for } T_i < t < T_i + \dfrac{D_i}{r_{corr}} \right) \\[2mm] 0 & \left(\text{for } t \geq T_i + \dfrac{D_i}{r_{corr}} \right) \end{cases} \tag{7}$$

where $A(t)$ is the effective cross-sectional area of a steel bar, D_i is the diameter of the undamaged steel bar, T_i is the corrosion onset time, r_{corr} is the rate of corrosion reflecting both the thickness of the concrete cover and the water-cement ratio, and $D(t)$ is the effective diameter of the steel bar after the lapse of t years. In addition, the effective diameter $D(t)$ is expressed using the following equation

$$D(t) = D_i - r_{corr} \times (t - T_i) \tag{8}$$

It is assumed in Eq. (8) that corrosion starts to occur and to reduce the steel bar diameter after time T_i. When introduced to the finite element model, the time-varying cross sectional area of the steel bars can simulate steel corrosion.

In addition to the corrosion-induced structural deterioration model, material nonlinearity is also considered for simulating more realistic behavior. A variety of models have been developed to represent the nonlinear behavior of construction materials such as concrete and steel, and it is important to employ their material property curves that are actually used for the construction of the target bridge. To account for material nonlinearity in this study, the strain-stress curves of concrete and steel rebar are selected after investigating the design drawing of the example bridge, which is

described in the later section. Furthermore, these nonlinear models for steel rebar and concrete enable the acquisition of a limit-state defined by the displacement ductility demand, which is also described later.

3.3 Software platform

For the proposed framework, a new software platform aimed at efficient fragility analysis is built by combining three components: (1) FERUM for reliability analysis, (2) ABAQUS for structural analysis with the finite element model, and (3) a Python-based interface for FERUM and ABAQUS (PIFA), as shown in Fig. 3. Developed at the University of California Berkeley, FERUM is a MATLAB-based open source package for reliability analysis (Sudret and Der Kiureghian 2000). ABAQUS is a commercial software package for finite element analysis. Combined use of FERUM and ABAQUS (also called FERUM-ABAQUS) enables a time-efficient structural reliability analysis that can handle a detailed finite element model of a full-scale structure in conjunction with FORM.

FERUM-ABAQUS was reported as being an effective and viable tool for structural reliability analysis through its applications to an aircraft wing (Lee *et al.* 2008) and a bridge pylon (Kang *et al*.). In these applications, the limit-states were defined by yielding and material nonlinearity was not considered; however, the nonlinear behavior of construction materials should be addressed in finite element analysis for accurate flood fragility analysis. However, this requires a computationally effective interface between FERUM and ABAQUS. For this reason, an interface, termed PIFA, is newly developed in this study.

PIFA is carefully designed in this study to control the overall process of reliability analysis efficiently, through interaction with FERUM and ABAQUS. Once uncertainty information is provided for FERUM and the reliability analysis employing FORM begins, the first task of PIFA is to create an input file for ABAQUS (i.e., in the "*.inp" file format written in Python language).
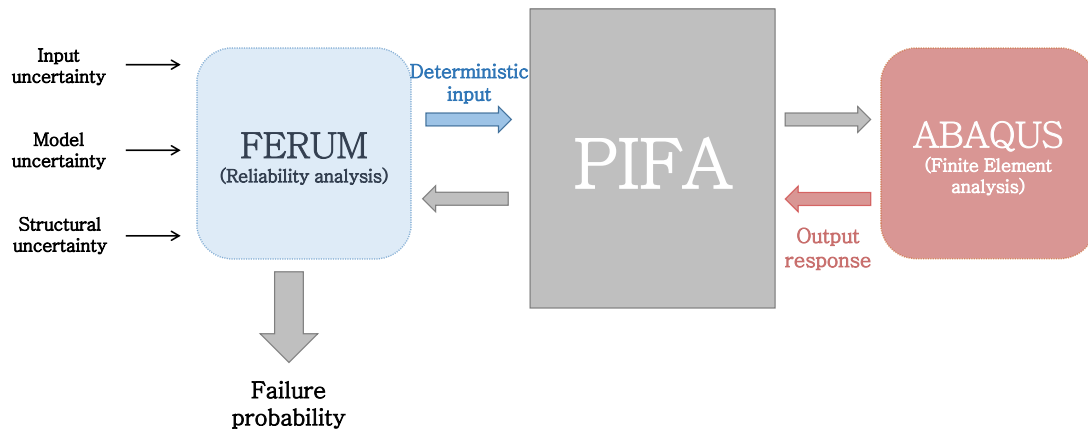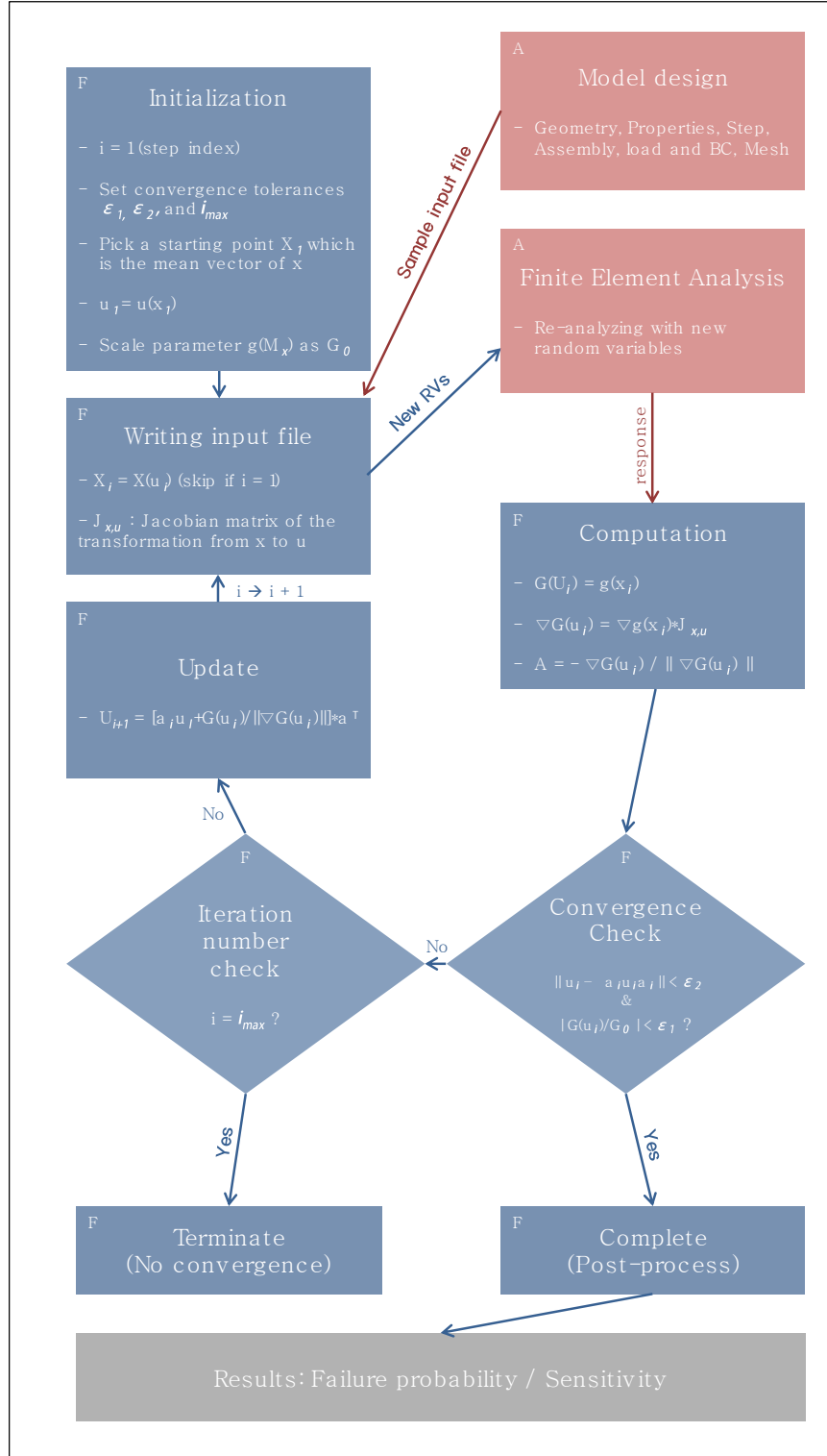

Fig. 3 Software platform

Fig. 4 FORM analysis employing the newly developed software platform

It contains geometry information of the analytical model, material properties, analysis time steps, locations of each part, load or boundary conditions, and meshing information. From among these data, users can select uncertainty factors (i.e., RVs), whose values depend on their statistical characteristics. Using the input file, ABAQUS performs finite element analysis and returns output responses such as stress or displacement. After the completion of finite element analysis, reading of ABAQUS outputs from nonlinear finite element analysis may take a long time because structural responses are obtained at many time steps due to the nature of nonlinear finite element analysis. In the previous applications of FERUM-ABAQUS, an interface code built on MATLAB was responsible for writing inputs and reading outputs, which took a relatively long time. To save time, a new interface code between FERUM and ABAQUS, termed PIFA, is developed in this research. PIFA enables access of the "*.odb" file, which is the output data base of ABAQUS, and the acquisition of the target structural response much more effectively. These responses are returned once more to FERUM so that it can enter the next iteration step. After the repetition of these iterative steps until convergence, the final result of failure probability is obtained. This process is explained by means of a flow chart in Fig. 4.

4. Example application of proposed framework

As an application example, the proposed framework of flood fragility analysis for bridges is applied to the Wolam Bridge, which is an actual bridge located in South Korea traversing a tributary of the Nakdong River. On the basis of the structural design drawing of the bridge, a finite element model is built for flood fragility analysis using the proposed framework. The detailed process of the application of the proposed fragility analysis framework employing the finite element model is described in this section.

4.1 Wolam Bridge

The Wolam Bridge, shown in Fig. 5, is 30-meter broad and 63-meter long reinforced concrete (RC) bridge. The design strengths of pier concrete and steel rebar are respectively 23.5 [MPa] and 294.2 [MPa], and the rebar diameter is 20 [mm]. The bridge consists of slab, abutment, pier and mass concrete located between slab and piers; The slab is not connected to the pier directly, but it puts on the mass concrete. The bridge was designed in compliance with the Korea Highway Bridge Design Specification (KHBDS) and its construction was completed in 2005. In dry seasons, its water level is relatively low, as shown in Fig. 5. However, the water level can potentially exceed the level of the girders and the water streams fast in the case of floods, which is the assumed flood scenario with this example.

As shown in Fig. 6, the ABAQUS finite element model of the bridge was established on the basis of its original structural design. It is shown in this design that the piers of the bridge are largely aligned in three rows, with each row consisting of eight piers symmetrically aligned on the front and rear sides (four each), forming six pier groups in total. Because all pier groups are weakly connected to the deck with isolation bearings, each pier system can be considered to behave independently under the water pressure. A pier group with the maximum stress and displacement is selected to increase computational efficiency through preliminary analysis employing the mean values of RVs, and as shown in Fig. 6, the one in the center at the upstream side is utilized in the fragility analysis. It should be noted that the pier groups have long

foundations in the direction of the water flow; thus, bridge scour is not expected to cause structural failures.
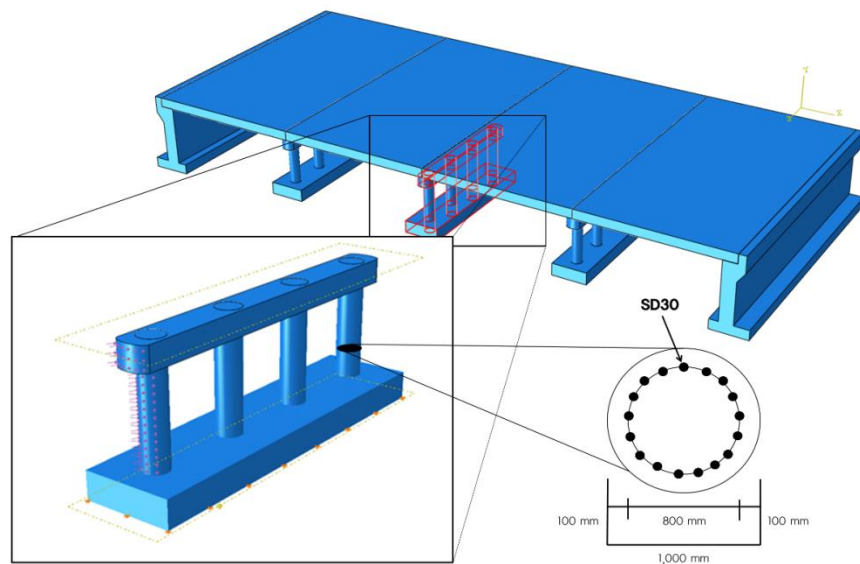

Fig. 5 Wolam Bridge

Fig. 6 ABAQUS model of Wolam Bridge

The pier group consists of a top concrete layer, four RC piers, and a bottom concrete base. The schematic at the bottom-right corner of Fig. 6 shows the cross-section of one RC pier having a diameter of 1,000 mm, of which 100 mm is the thickness of the concrete cover, and SD30 was used as the steel bar material. The strain-stress curves of the concrete and steel bar shown in Fig. 7 are introduced in order to account for their material nonlinearities, and these strain-stress curves are respectively obtained from Le Roux and Wium (2012) and Shima and Tamai (1987) after a comprehensive literature review. In addition, preliminary analysis using the water pressure expressed in Eq. (6) revealed that the first upstream-side pier incurred substantially higher stress and displacement than the remaining three piers. On the basis of this result, this study focuses on the analysis of the first pier. It is also assumed, as shown at the bottom-left corner of Fig. 6, that the water pressure is applied to the entire perpendicular section to the water flow, as expected in actual floods. In addition, vehicle load is not considered because it is assumed that the bridge is fully inundated and vehicles cannot pass on the bridge.

4.2 Statistical parameters

In this application example, three kinds of uncertainties are considered and assumed as RVs: elastic modulus (i.e., Young's modulus), mass density, and water pressure intensity. The first kind of uncertainty characterizes the uncertainty of the material property, and the second one accounts for the uncertainty of the bridge self-weight. The uncertainty of water pressure is considered by the introduction of water pressure intensity which is multiplied with the water pressure p in Eq. (6). It is assumed in this example that the RVs are statistically independent each other. The statistical properties (i.e., mean, standard deviation, and probability distribution type) of the RVs are determined based on a comprehensive literature survey (Lehký *et al*. 2012, Ju *et al.* 2014, Kolisko *et al.* 2012), and they are summarized in Table 2.

4.3 Limit-states

In this study, the flood fragility analyses are based on nonlinear finite element analysis. The derivation of the fragility curves requires calculating the conditional probability that the example bridge undergoes different levels of structural damage under certain levels of flood intensity, which is not an easy task. In addition, owing to the effects of structural deterioration induced by corrosion, the fragility curves should be updated during the bridge lifetime. These aspects make it difficult to define the limit-states for the proposed framework.

Table 2 Statistical properties of RVs

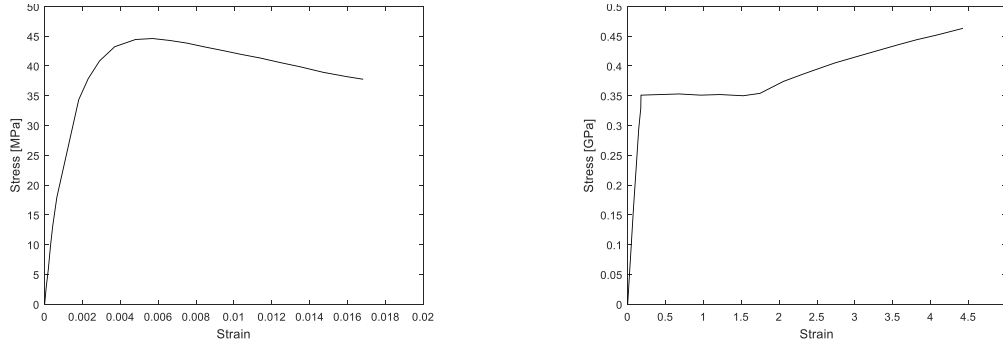|	Mean	Standard deviation	Coefficient of variation	Distribution type
Concrete mass density	2,300 [kg/m^3]	115 [kg/m^3]	0.05	Normal
Concrete elastic modulus	26.9 [GPa]	2.46 [GPa]	0.0917	Normal
Steel bar mass density	7862.3 [kg/m^3]	314.5 [kg/m^3]	0.04	Normal
Steel bar elastic modulus	190 [GPa]	1.9 [GPa]	0.01	Normal
Water pressure intensity	1	0.1	0.10	Normal

Fig. 7 Strain-stress curves of concrete (left) and rebar (right)

Recently, Dong *et al*. (2013) defined four different damage states of seismic damage of a bridge based on the basis of the ductility demand of columns and successfully derived the seismic fragility curves of a bridge in consideration of structural deterioration. In their research, ductility was defined in terms of displacement, and the displacement ductility demand M_D, a measure of the plastic deformation on a component, was calculated as (Caltrans 2006)

$$M_D = \Delta_D / \Delta_Y \tag{9}$$

where Δ_D is the displacement under a certain level of load and Δ_Y is the yield displacement to the formation of a plastic hinge. An M_D value of 1 means that the displacement does not reach the yielding level. On the other hand, if an M_D value is greater than 1, it means that the structure enters the plastic range. Experimental results of Caltrans (2006) give the target displacement ductility depending on the type of bridge model, as presented in Table 3. From the perspective of structural analysis, the lateral hydraulic loadings due to water flow are essentially similar to that due to horizontal ground motion; therefore, the displacement ductility demand specified in Caltrans (2006) can be considered appropriate for use in the present study. The Wolam Bridge has long foundations in the direction of water flow, and the foundation can be assumed to be a fixed boundary condition in the structural analysis. Thus, the target displacement ductility demand for defining a complete failure (i.e., collapse) is assumed to be 5.0 from Table 3, in accordance with the structural type of the Wolam Bridge.

Table 3 Displacement ductility demand (Caltrans 2006)

Single column bents supported on fixed foundation	$M_D \leq 4$
Multi-column bents supported on fixed or pinned footings	$M_D \leq 5$
Pier walls (weak direction) supported on fixed or pinned footings	$M_D \leq 5$
Pier walls (strong direction) supported on fixed or pinned footings	$M_D \leq 1$

Table 4 Damage states and corresponding ductility demands (Dong *et al.* 2013)

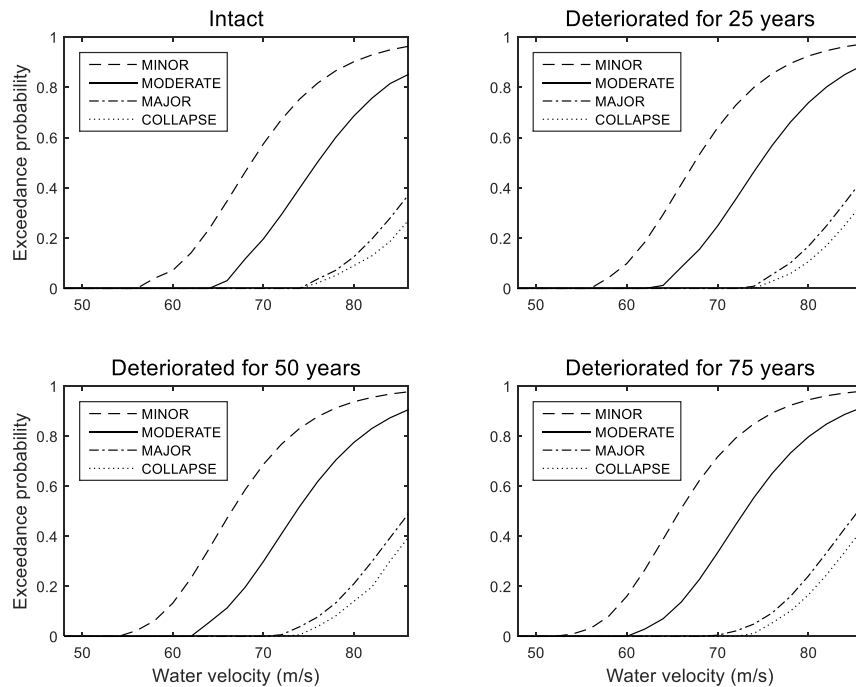| Damage state	*Ductility demand*
Minor damage	$1 \leq M_D \leq 2.9$
Moderate damage	$2.9 \leq M_D \leq 4.6$
Major damage	$4.6 \leq M_D \leq 5.0$
Collapse	$M_D > 5.0$

Fig. 8 Flood fragility curves for various damage states

In addition to the damage state of collapse, Dong *et al.* (2013) defined three more damage states by use of the ductility demand: minor, moderate, and major damage states. The definitions of these damage states are summarized in Table 4, and all four damage states are applied to the bridge example.

4.4 Analysis result: flood fragility curves

Using the proposed framework, fragility analysis of the Wolam Bridge against floods is conducted, and the corresponding analysis results are shown in Figs. 8 and 9. In accordance with

the displacement ductility demands defined in Table 4 and the structural deterioration model described in Section 3.2, flood fragility curves are derived with four damage states and four different time points.

First, it is seen in Fig. 8 that the exceedance probability of a certain damage state increases with increasing water velocity. This is natural because, as expressed in Eq. (6), the water pressure increases quadratically with increasing water velocity. In addition, it is observed that the exceedance probability increases with aging of the bridge. For a clearer demonstration of this trend, Fig. 9 is plotted to present the flood fragility curves for various time instants (i.e., intact, 25 years, 50 years, and 75 years). For example, the conditional probability of exceeding the moderate damage state under a water velocity of 70 m/s is initially about 0.197; however, this value becomes 0.335 at $t = 75$ years. This is due to the effects of structural deterioration induced by corrosion. As described in Eqs. (7) and (8), corrosion deteriorates a structure by decreasing its effective area and thus reducing its stiffness.

Finally, it is also noticed from Figs. 8 and 9 that the level of water velocity at which the flood fragilities have meaningful values of exceedance probability is slightly higher. Compared to the usual range of water velocity in a flood, which is from 3 m/s to 10 m/s, the water velocities in Figs. 8 and 9 may appear relatively unrealistic. This may be because, for the sake of simplicity, scour which is one of the representative causes of flood-induced bridge failure is not considered in this example. However, a bridge's failure is generally an extremely rare event, and it still requires proper mitigation and preparedness actions according to the flood fragility curves. From this viewpoint, the proposed framework can aid in taking such actions, especially for bridges that are much more vulnerable to floods than is the Wolam Bridge.
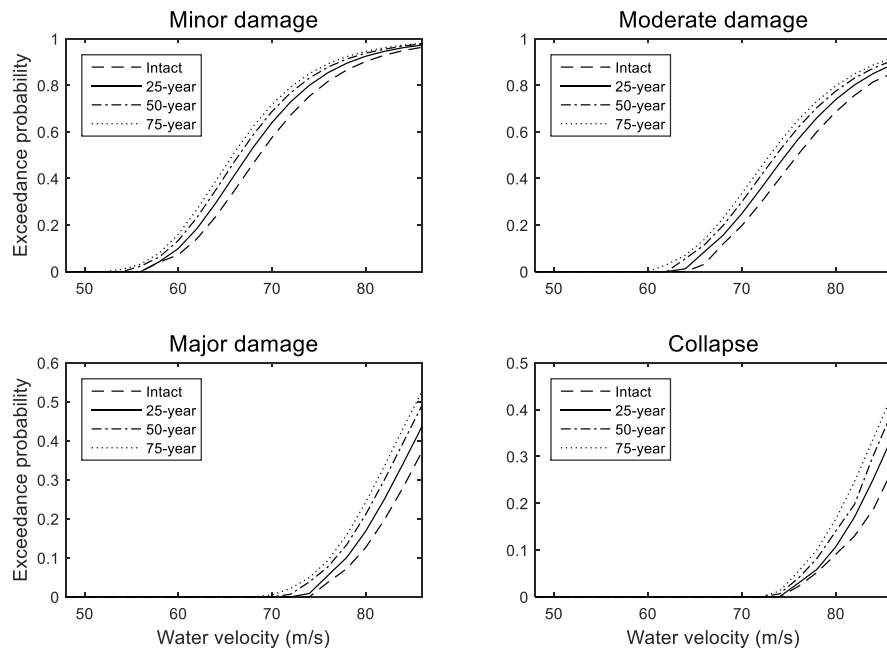

Fig. 9 Flood fragility curves for various time instants

5. Conclusions

This study developed a novel methodology for the derivation of flood fragility curves for bridges, in consideration of structural deterioration. Although bridges are prone to be damaged by floods, only a few previous studies have focused on flood fragility analysis. Since the flood-induced failure of bridges is affected by various hydraulic factors such as water pressure, debris, and corrosion, as well as the nonlinear behavior of construction materials, the proposed framework provides a way of modeling the hydraulic factors and the material nonlinearity in the finite element model. In addition, for more effective flood fragility analysis, a new software platform was built by combining the following three components: (1) FERUM for reliability analysis, (2) ABAQUS for finite element analysis, and (3) a Python-based interface for FERUM and ABAQUS, termed PIFA. The new platform enables to perform reliability analysis in conjunction with sophisticated finite element analysis. The proposed framework including the new platform was applied to the Wolam Bridge, which is an actual RC bridge in Korea. The analysis results revealed that the flood fragilities increased with increasing water velocity in a flood event. The results also showed that the exceedance probabilities of damage states increased with the aging of the bridge and with its deterioration due to corrosion. These results confirm the successful application of the proposed framework to the derivation of flood fragility curves for bridges.

Acknowledgements

References

AASHTO. (2012), *AASHTO LRFD Bridge Design Specifications*, 6th Ed., Washington, DC.

Caltrans. (2006), *Seismic Design Criteria*, California DOT: Sacramento, California.

Dawson, R., Hall, J., Sayers, P., Bates, P. and Rosu, C. (2005), "Sampling-based flood risk analysis for fluvial dike systems", *Stochastic Environmental Research and Risk Assessment*, **19**(6), 388-402.

Decò, A. and Frangopol, D.M. (2011), "Risk assessment of highway bridges under multiple hazards", *J. Risk Res.*, 14(9), 1057-1089.

Der Kiureghian, A. (2005), *First- and second-order reliability methods*, Engineering Design Reliability Handbook, (Eds., Nikolaidis, E., Ghiocel, D.M. and Singhal, S.), CRC Press, Boca Raton, FL, USA, Chapter 14.

Dong, Y., Frangopol, D.M. and Saydam, D. (2013), "Time-variant sustainability assessment of seismically vulnerable bridges subjected to multiple hazards", *Earthq. Eng. Struct. D.*, **42**(10), 1451-1467.

Ghosn, M., Moses, F. and Wang, J. (2003), *Design of highway bridge for extreme events*, NCHRP Report 489, Transportation Research Board, Washington, D.C.

Haldar, A. Ed. (2006), *Recent Developments in Reliability-based Civil Engineering*, World Scientific Publishing Company Incorporated, Singapore.

Johnson, P.A. (1996), "Uncertainty of hydraulic parameters", *J. Hydraul. Eng. - ASCE*, **122**(2), 112-114.

Johnson, P.A. and Dock, D.A. (1998), "Probabilistic bridge scour estimates", *J. Hydraul. Eng. - ASCE*, **124**(7), 750-754.

Ju, M., Oh, H. and Sun, J.W. (2014), "Simplified reliability estimation for optimum strengthening ratio of

30-year-old double T-beam railway bridge by NSM techniques", *Mathematical Problems in Engineering*, 2014, 734016.

Kang, W.H., Lee, Y.J., Song, J. and Gencturk, B. (2012), "Further development of matrix-based system reliability method and applications to structural systems", *Structure and Infrastructure Engineering: Maintenance, Management, Life-cycle Design and Performance*, **8**(5), 441-457.

Kolisko, J., Hunka, P. and Jung, K. (2012), "A statistical analysis of the modulus of elasticity and compressive strength of concrete C45/55 for pre-stressed precast beams", *J. Civil Eng. Architect.*, **6**(11), 1571-1576,

Korea Road & Transportation Association (2010), *Korean Highway Bridge Design Specification (KHBDS)*, Ministry of Land, Transport and Maritime Affairs of Korea, Seoul (in Korean).

Le Roux, R.C. and Wium, J.A. (2012), "Assessment of the behaviour factor for the seismic design of reinforced concrete structural walls according to SANS 10160-part 4: technical paper", *J. South African Inst. Civil Eng.*, **54**(1), 69-80.

Lee, Y.J. and Moon, D.S. (2014), "A new methodology of the development of seismic fragility curves", *Smart Struct. Syst.*, **14**(5), 847-867.

Lee, Y.J., Song, J. and Tuegel, E.J. (2008), "Finite element system reliability analysis of a wing torque box", *Proceedings of the 10th AIAA Nondeterministic Approaches Conference*, April 7-10, Schaumburg, IL., USA.

Lehký, D., Keršner, Z. and Novák, D. (2012), "Determination of statistical material parameters of concrete using fracture test and inverse analysis based on FraMePID-3PB tool", *Proceedings of the 5th International Conference on Reliable Engineering Computing (REC 2012)*, Brno, Czech Republic.

Melchers, R.E. (1999), *Structural Reliability: Analysis and Prediction*, (2nd Ed.), John Wiley & Sons, New York, NY, USA.

Schmocker, L. and Hager, W.H. (2011), "Probability of drift blockage at bridge decks", *J. Hydraul. Eng. - ASCE*, **137**(4), 470-479.

Shima, H. and Tamai, S. (1987), "Tension stiffness model under reversed loading including post yield range", *International Association for Bridge and Structural Engineering*, Colloquium, Lisbon, Portugal.

Song, J. (2007), *Decision and Risk Analysis*, *Lecture Notes*, University of Illinois at Urbana-Champaign, Urbana, IL, USA, Feb. 28.

Sudret, B. and Der Kiureghian, A. (2000), *Stochastic finite element methods and reliability*, A State-of-the-Art Report, Report No. UCB/SEMM-2000/08, Department of Civil and Environmental Engineering, University of California, Berkeley.

Thoft-Christensen, P., Jensen, F.M., Middleton, C.R. and Blackmore, A. (1997), "Revised rules for concrete bridges", *Safety of Bridges, The Institution of Civil Engineers*, Thomas Telford, 175-188.

Vu, K.A.T. and Stewart, M.G. (2000), "Structural reliability of concrete bridges including improved chloride-induced corrosion models", *Struct. Saf.*, **22**(4), 313-333.

Wardhana, K. and Hadipriono, F.C. (2003), "Analysis of recent bridge failures in the United States", *J. Perform. Constr. Fac.*, **17**(3), 144-150.

Witzany, J. and Cejka, T. (2007), "Reliability and failure resistance of the stone bridge structure of Charles Bridge during floods", *J. Civil Eng. Management*, **13**(3), 227-236.